Planetary and Space Science 86 (2013) 150–154

Contents lists available at ScienceDirect

Planetary and Space Science

journal homepage: www.elsevier.com/locate/pss

Dielectric and hardness measurements of planetary analog rocks in support of in-situ subsurface sampling

Ahmed ElShafie [a], Essam Heggy [b,*]

[a] Arkansas Center for Space and Planetary Sciences, University of Arkansas Fayetteville, AR 72701, USA
[b] Jet Propulsion Laboratory, California Institute of Technology, Pasadena, CA 91109, USA

ARTICLE INFO

Article history:
Received 7 June 2012
Received in revised form
8 November 2012
Accepted 12 February 2013
Available online 26 March 2013

Keywords:
Hardness
Dielectric properties
Subsurface sampling
Drilling
Mars
Planetary surfaces

ABSTRACT

Accurate assessment of the subsurface mechanical characteristics and how they correlate with dielectric properties is crucial to optimize future drilling and sampling investigations on planetary bodies. For 12 different types of basaltic rocks with different hardnesses, we use capacitive cells to measure the real part of the dielectric constant over the frequency range 100–1000 MHz, and a Schmidt hammer hardness tester to measure the hardness using a scale of 10–100. Our measurements suggest that the real part of the dielectric constant and rock hardness are linearly correlated. Additionally, sample hardness was linearly correlated to density. For a density ranging from 0.82 to 3.05 g/cm^3, the real part of the dielectric constant ε' and rebound hardness values R ranged from $\varepsilon'=1.8$–7.6 and $R=14.16$–68 for the different basalt samples. Hence, high dielectric constants imply a high rock hardness value and vice versa. We concluded that for volcanic surfaces that are analogous to the Martian surface as well as other planetary surfaces, there is an inverse correlation between drilling penetration rate based on the rotary-percussive drill method and the dielectric constant. Dielectric inversion from planetary radar probing experiments proposed herein is a crucial method to locate regions with lowest hardness and hence highest drilling penetration rate in desiccated volcanic planetary subsurfaces. The use of these cross-correlation measurements can optimize future drilling experiments and ensure that they reach their targets of opportunities, minimize losses in drilling performance, or the unnecessary use of power that will be needed for the continuity of the investigation.

1. Introduction

Dielectric properties, $\varepsilon=\varepsilon'-i\varepsilon''$ (i.e., the real (ε') and imaginary parts (ε'') of the dielectric constant), as inverted from radar subsurface sounding data (e.g., Boisson et al., 2011; Alberti et al., 2012), are increasingly suggested to assess the ground mechanical properties of rock hardness, density, and porosity for several planetary surfaces. Of a particular interest is the in situ sampling from Mars, comets, asteroids, and icy satellites, as their shallow subsurfaces hold a key information for understanding the volatiles occurrence, geological evolution, and geophysical properties of these planetary bodies. Conjugating penetrometers and/or drills with sounding radars have been widely suggested to optimize subsurface investigation and sampling (e.g., Kofman and Safaeinili, 2004; Heggy et al., 2012). For example, the Rosetta lander will use the Comet Nucleus Sounding Experiment by Radiowave Transmission (CONSERT) radar sounder—supporting the Multi-Purpose Sensors for Surface and Subsurface Science (MUPUS) penetrometer and the Sample and Distribution Device (SD^2) drill—to probe the subsurface of comet 67P/Churyumov–Gerasimenko and to identify localities of high scientific return with minimum drill and penetration risk (Biele, 2002). Moreover, the proposed Ground Penetrating Radar (GPR) experiment Water Ice Subsurface Deposit Observation on Mars (WISDOM) will support the ExoMars rover's drill to perform subsurface sampling on Mars (Ciarletti et al., 2009). In addition, drilling and subsurface sample returns have also been suggested for asteroid missions (Lauretta and Team, 2012) to understand subsurface mineralogical properties that can provide an insight to the differentiation mechanisms and the shock history of these bodies. In all these different planetary surfaces, the drilling capabilities strongly depend on identifying optimal locations where rock hardness permits penetration to the subsurface samples of interest. Radargrams from orbiting or ground penetrating radars can identify the locations where observed anomalous dielectric constants can suggest subsurface inclusion of ice and porous materials (Heggy et al., 2003; Campbell et al., 2009; Mouginot et al., 2012). Hence, an accurate assessment of the subsurface mechanical properties—i.e., rock hardness, density and porosity—and how they correlate to dielectric properties is crucial in optimizing future drilling investigations.

While the porosity and density dependency of the dielectric properties of planetary analogs have been explored (e.g., Olhoeft and Strangway, 1975; Ulaby et al., 1990; Rust et al., 1999; Heggy et al., 2001), the dependency on rock hardness remains poorly

* Corresponding author. Tel.: +1 818 393 7895.
E-mail address: heggy@jpl.nasa.gov (E. Heggy).

0032-0633/$ - see front matter © 2013 Elsevier Ltd. All rights reserved.
http://dx.doi.org/10.1016/j.pss.2013.02.003

understood for volcanic materials, which are considered to be the most accurate analog to planetary surfaces. Such ambiguities compromise the accuracy of the dielectric inversion to estimate the ground hardness, reducing the performance of the drill and potentially missing or altering targets of interest.

Therefore, the main purpose of this research is to measure the real part of the dielectric constant and rock hardness for planetary analog desiccated volcanic rocks to provide a cross-relation between these two subsurface parameters. These findings will significantly improve our ability to perform dielectric inversion from past, present, and future radar experiments to assess the subsurface rock hardness to support, locate and optimize the drill operation for sampling purposes, as well as to characterize the physical properties of the shallow subsurface.

2. Experimental method and sample description

2.1. Sample preparation and measurements procedure

We used 12 different samples of volcanic rocks for dielectric and hardness measurements: eight consolidated basaltic rocks (Belleville basalt, Somerset basalt, Flood basalt, Saddleback basalt, Olivine basalt, Crater of the Moon AA lava (COM-AA), Crater of the Moon PHOE lava (COM-PHOE) and Crater of the Moon Tephra (COM-TH)) and four pyroclastics (Crater of the Moon Welded Tuff (COM-WTUFF), Crater of the Moon Pumice (COM-Pumice), Bishop Welded Tuff (BIS-WTFF) and Bishop Un-welded Tuff (BIS-UTFF)) from seven different locations in Belleville, NV; Valmont, CO; Somerest, NJ; Pullman, WA; Saddleback, CA; Bishop, CA; and Butte, ID. These samples were all identified as Martian analogs. These 12 samples were chosen for their Martian analogy in term of their compositional and petrophysical properties (Heggy et al., 2006; Grimm et al., 2006). Our samples have a comparable enrichment in iron ~14% and titanium ~3%; this will help to de-convolve any changes in the dielectric properties that could arise from different iron concentrations (Olhoeft, 2000). For each sample, we cut a core and thinly sliced the specimens to perform hardness and dielectric measurements on the same sample. We determined the density of dielectric and hardness samples using the same measurement technique for each rock sample. Using a scale with a measurement accuracy of 0.001 g, we measured the masses for each sample. Volume measurements are performed using the fluid immersion technique of the samples into a filled graduated cylinder. The difference in fluid volume is a direct measurement of the sample volume. We then divided the measured mass for each sample by its measured volume to determine the density of each sample.

The dielectric constant of volcanic rocks can change substantially as a function of residual moisture content (Olhoeft and Strangway, 1975). Telluric planetary surfaces are highly desiccated; therefore, our dielectric and hardness measurements are carried out on desiccated samples at room temperature. Desiccation is carried out by oven heating the samples for 48 h at 80 °C to eliminate the residual moisture as listed in Tables 1 and 2.

2.2. Hardness measurements

Hardness is a measure of the resistance of material when it is under confined stress; hardness values identify how well the material overcomes the mineral constituents of the rock as well as the bond strength that exists between the mineral grains (Parkhomenko and Keller, 1967). The mechanical behavior of volcanic rocks under stress forces is complex; therefore, there are different experimental techniques for measuring samples hardness: scratch, indentation, and rebound hardness (Atkinson et al., 1978).

Table 1
Schmidt hammer hardness and density measurements of different desiccated volcanic rock samples.

Rock types	Location	Moisture content before desiccation % in mass	Density, ρ (g/cm^3)	Schmidt hammer hardness (R)	Standard deviation
Belleville basalt	Belleville, NV	0.51	2.93 ± 0.07	66.43	3.7
Somerset basalt	Somerset, NJ	0.72	3.05 ± 0.07	64.45	2.8
Flood basalt	Pullman, WA	0.79	3.01 ± 0.10	68	2.9
Saddleback basalt	Saddleback, CA	0.65	2.65 ± 0.03	61.2	3.4
Olivine basalt	Valmont, CO	0.19	3.00 ± 0.02	67.9	2.5
COM-WTUFF	Butte, ID	0.35	1.86 ± 0.03	33.37	2.8
COM-Pumice	Butte, ID	1.33	0.82 ± 0.07	14.16	2.2
COM-PHOE	Butte, ID	0.29	2.23 ± 0.02	40.67	1.9
COM-AA	Butte, ID	0.13	2.28 ± 0.02	42.56	2.3
COM-TH	Butte, ID	0.23	1.13 ± 0.06	16.26	2.0
BIS-WTFF	Bishop, CA	0.15	1.46 ± 0.02	26.32	2.4
BIS-UTFF	Bishop, CA	0.22	1.21 ± 0.06	22.11	1.5

We perform hardness measurements for desiccated samples using the rebound technique, as it is a non-destructive technique that does not leave any imprints on the test sample and is sensitive in differentiating the hardness between two samples that have close density values (Hucka, 1965; Ericson, 2004; Goudie, 2006). We use the Proceq Schmidt hammer type-L with hammer impact energy of 0.735 N m. Core specimens are checked to ensure that they are free of visible cracks and that they are the representative of the rock mass. For data collection, 10 rebound tests are recorded per sample and averaged to determine the rebound number R with a repeatability of ~1.5—4% as observed in the standard deviations values for hardness in Table 1.

2.3. Dielectric measurements

Laboratory dielectric measurements of thinly sliced, desiccated samples < 3 mm in thickness are carried out at room temperature using a dielectric capacitive cell and a test fixture attached to an impedance analyzer. The analyzer is connected to a central command unit to extract data and to calculate, in real-time, the real and imaginary parts of the complex dielectric constant. Samples are placed between the parallel plates of a guarded capacitive cell to reduce edge errors. Sweeping over the frequency range of observation and knowing the thickness of the sample, we can calculate the real and imaginary parts of the dielectric constant from the capacitance and admittance. Values of the dielectric constant are measured over the entire frequency range, 100–1000 MHz, thereby covering the frequency ranges of several previous, current, and future sounding radar experiments. The full description of the dielectric measurement setup and sample preparation can be found in Heggy et al. (2001, 2012).

3. Results and discussion

For desiccated samples, the Schmidt hammer rebound hardness ranged from $R = 14.16$ to $R = 68$ at densities between 0.8 g/cm^3 and 3 g/cm^3 for COM-Pumice and Flood basalt, respectively (Table 1). The lowest and highest R values (i.e., for COM-Pumice

Table 2
Dielectric measurements of volcanic rocks for desiccated and un-desiccated samples.

Rock types	Moisture (%)	Density, ρ (g/cm^3)	ε' (100 MHz)[a]	ε' (500 MHz)[a]	ε' (1 GHz)[a]	ε' (100 MHz)[b]	ε' (500 MHz)[b]	ε' (1 GHz)[b]
Belleville basalt	0.37	2.93 ± 0.07	8.56	7.89	7.73	7.53	7.35	7.34
Somerset basalt	1.01	3.05 ± 0.07	10.29	10.65	10.26	7.88	7.68	7.66
Flood basalt	0.92	3.01 ± 0.10	10.11	8.7	8.25	7.81	7.57	7.14
Saddleback basalt	0.15	2.65 ± 0.03	8.73	8.16	7.92	7.56	7.29	7.25
Olivine basalt	0.12	3.00 ± 0.02	9.16	8.7	8.54	7.75	7.66	7.69
COM-WTUFF	0.33	1.86 ± 0.03	3.06	3.03	3.02	2.58	2.57	2.57
COM-Pumice	1.07	0.82 ± 0.07	1.95	1.94	1.94	1.88	1.87	1.86
COM-PHOE	0.1	2.23 ± 0.02	4.73	4.58	4.49	4.56	4.41	4.31
COM-AA	0.13	2.28 ± 0.02	7.82	7.13	6.81	7.43	6.80	6.43
COM-TH	0.23	1.13 ± 0.06	5.72	5.63	5.24	5.45	5.23	4.94
BIS-WTFF	0.15	1.46 ± 0.02	6.54	6.22	6.01	5.92	5.84	5.71
BIS-UTFF	0.22	1.21 ± 0.06	4.90	4.72	4.33	4.33	4.24	4.01

[a] Undesiccated.
[b] Desiccated.

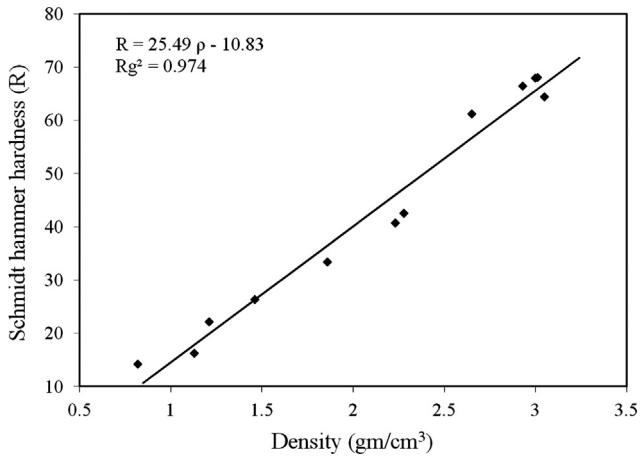

Fig. 1. Schmidt hammer hardness number (R) versus sample bulk density for desiccated volcanic rocks from Table 1.

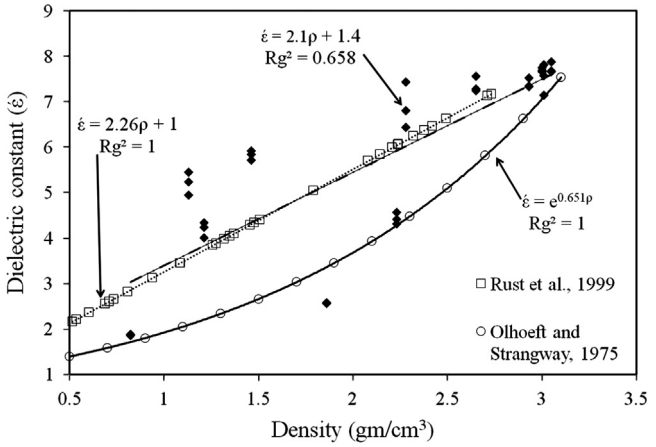

Fig. 2. Dielectric constant of volcanic rocks as a function of sample bulk density from Table 2 and fitted model curves by Olhoeft and Strangway (1975) and Rust et al. (1999).

and flood basalt) correspond to the lowest and highest densities of the samples. All results of Schmidt hammer hardness tests are within the standard deviation (minimum of 1.5 to maximum of 3.7).

For volcanic materials used in this study, the residual moisture is observed to have no significant impact on rock hardness. For volcanic rocks, we observe that as the sample density increases, the hardness also increases, which suggest a correlation between the density and hardness measurements, as observed in the linear trend of the laboratory measurement data interpolation with a regression coefficient, $Rg^2 = 0.97$ in Fig. 1. We empirically model the above-mentioned dependency using Eq. (1), which describes the function between the Schmidt hammer hardness number (R) and the material density (ρ).

$$R = (25.49\rho) - 10.83 \quad (1)$$

Dielectric measurements for un-desiccated and desiccated samples with a given density are listed in Table 2 at three frequency ranges (100 MHz, 500 MHz, and 1 GHz). Desiccation is observed to decrease the real part of the dielectric constant with different amplitudes for the different samples due to the different moisture contents as well as the ionic interactions induced by the water presence in the samples. In the Somerset basalt, Flood basalt and COM-Pumice samples, desiccation eliminated the residual moisture, which constitutes 1.01%, 0.92%, and 1.07% of the sample masses, respectively; therefore the real part of the dielectric constant decreased from 10.29 to 7.88, 10.11 to 7.81, and 1.95 to 1.88 at a frequency of 100 MHz, corresponding to 23%, 22%, and 4% variations in Somerset basalt, Flood basalt, and COM-Pumice (Table 2). Such a variation is related to the presence of iron oxides in the samples (Heggy et al., 2001). We do not observe a significant change in the real part of the dielectric constant for the rest of the samples due to the minimal moisture content (0.1–0.37%) of the samples' masses. The real part of the dielectric constant is observed to decrease with increasing frequency and to increase with increasing density of the rock samples (Fig. 2). A similar increase in the dielectric constant as a function of sample density is also reported by Olhoeft and Strangway (1975), Ulaby et al. (1990), and Rust et al. (1999). Olhoeft and Strangway (1975) measured the dielectric constant and density of lunar rocks with 0.23–22% of FeO and 0.02–12.2% of TiO_2, while Rust et al. (1999) conducted the same measurements on dacitic lava flows with 2.05–10.62% of FeO and 0.47–2.44% TiO_2, which show the latest data set to be a closer fit to our laboratory measurements. For the purpose of comparison, we fit our dielectric constant/density data in Table 2 with the measurements performed by Olhoeft and Strangway (1975) and Rust et al. (1999). Numerical fits by Olhoeft and Strangway (1975) and Rust et al. (1999) are both based on a logarithmic and linear formula. Our data show a similar trend and values as Rust et al. (1999), due to the similar sample composition and the close iron–titanium percentages.

Fig. 3 shows the Schmidt hammer hardness number (R) as a function of the real part of the dielectric constant (ε') for volcanic rocks at room temperature after desiccating the Basaltic samples at 80 °C for 48 h. The Schmidt hammer hardness is observed to increase by increasing the real part of the dielectric constant for

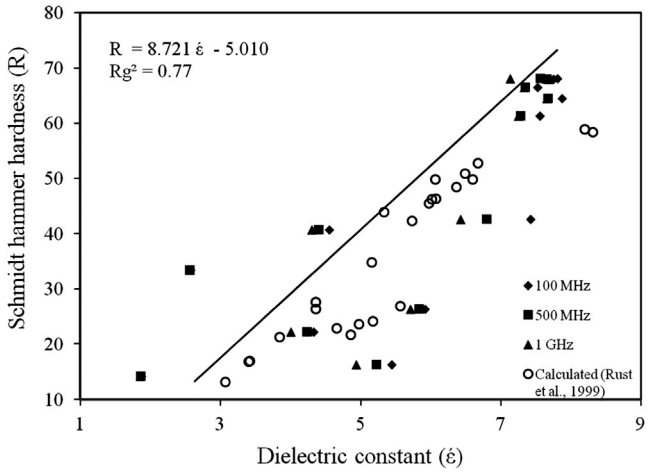

Fig. 3. Dielectric constant versus Schmidt hammer hardness number (R) of volcanic rocks for desiccated samples at different frequency ranges values from Tables 1 and 2 and the calculated Schmidt hammer hardness from Rust et al. (1999).

volcanic material (Fig. 3). To validate our approach, our results are compared to the calculated Schmidt hammer hardness number using Eq. (1) and the density values measured in Rust et al. (1999). Both measured and calculated hardnesses are in agreement, and suggest a linear correlation between the real part of the dielectric constant and the rebound hardness value for volcanic rocks. It is important to note that in Rust et al. (1999), dielectric constant and density measurements are conducted at a frequency of 10 MHz that is a close range for our experimental setup, especially when considering that volcanic rocks are non-dispersive and hence have very low frequency dependence in the range from 100 to 1000 MHz as shown in Table 2.

Parkhomenko and Keller (1967) propose an inverse relation between molecular polarizability and binding energy of minerals in sedimentary rocks, which suggests an inverse relationship between the dielectric constant and the hardness of minerals; hence the harder the mineral, the lower the dielectric constant. In contrast with Parkhomenko and Keller (1967), results on sedimentary rocks, our measurements suggest that for volcanic rocks and pyroclasts, the harder the rock, the higher the dielectric constant. A physical explanation for this linear correlation between the dielectric constant and the hardness in volcanic rocks is attributed to the density variations of the samples controlling this function and the absence of conductive mineral such as evaporates and clays. We observed that both hardness and the real part of the dielectric constant are linearly increasing with increased material density. Eq. (2) describes the linear correlation with a regression coefficient $Rg^2=0.77$, between the real part of the dielectric constant and rock hardness based on our laboratory measurements, with validation from Rust et al. (1999).

$$R=(8.721\varepsilon')-5.010 \quad (2)$$

While this empirical equation can be used to describe the real part of the dielectric constant–hardness function for volcanic rocks, it cannot be applied to sedimentary rocks, loose sediments, or icy surfaces. Further measurements will be needed to achieve that goal.

4. Implication for future planetary sampling experiments

Sampling planetary bodies provide an unique opportunity to understand their in-situ chemical and physical properties, which provides an insight into their formation history and evolution. The sampling capability is constrained by the surface hardness variability and the ability to retrieve low surface hardness locations to optimize drilling by reducing operational power and maximizing the platform stability. The amplitude of the gravity field defines the optimal sampling mechanisms for planetary bodies. At micro-gravity environments such as those found on asteroids and comets, techniques that anchor the surface and capture both surface and subsurface samples are considered to be the most effective, as suggested for the Rosetta mission. Additionally, other methods, such as firing the surface using bullets and collecting fragments, were successfully used on the Hayabusa mission. Drilling, penetrating, and harpooning the surface and collecting or casing samples are also suggested techniques for sampling a body with a substantial gravity field, such as a planet or its satellite. All the above-mentioned sampling techniques require interaction between the sampling device and the surface and the shallow subsurface. Feasibility of accessing and sampling is a function of the hardness of the investigated planetary body. Therefore, assessing the surface hardness on a large scale using dielectric inversion from radar probing can constrain drilling and sampling operational risks and maximizes the scientific return from properly targeting the subsurface. As suggested by our laboratory measurements, the real part of the dielectric constant can be used to estimate the surface and subsurface hardness values, which define the drilling rate to reach subsurface targets.

As hardness of a rock increases due to an increase in the rock density, the drill penetration rate (DPR) would decrease (Gstalder and Raynal, 1966). Kahraman et al. (2003) conducted the Schmidt hammer hardness and drill experiments on diabase, sandstone, dolomite, marl and limestone rocks using a rotary-percussive drill. The drill operation power was 14–17.5 kW with, with a bit diameter of 76–89 mm, a maximum Weight On Bit (WOB) of 600 N/cm^2, blow pressure and rotational pressure are of 100–120 bar and 60–70 bar respectively. We used Kahraman et al. (2003) DPR—the Schmidt hammer hardness relation in Eq. (3) to estimate the drill penetration rate for our samples.

$$\mathrm{DPR}=(-0.037R)+3.11 \quad \text{(Kahraman et al., 2003)} \quad (3)$$

Fig. 4 shows the calculated drill penetration rate (DPR) in meters per hour (m/h) as a function of the dielectric constant. A decrease in the DPR is observed with the increase in both rock hardness and dielectric constant as shown in Eq. (3) and Fig. 4. Eq. (4) suggests the linear correlation between DPR using a rotary-percussive drill and dielectric constant for volcanic rocks with a regression coefficient, $Rg^2=0.72$

$$\mathrm{DPR}=(-0.351\varepsilon')+3.636 \quad (4)$$

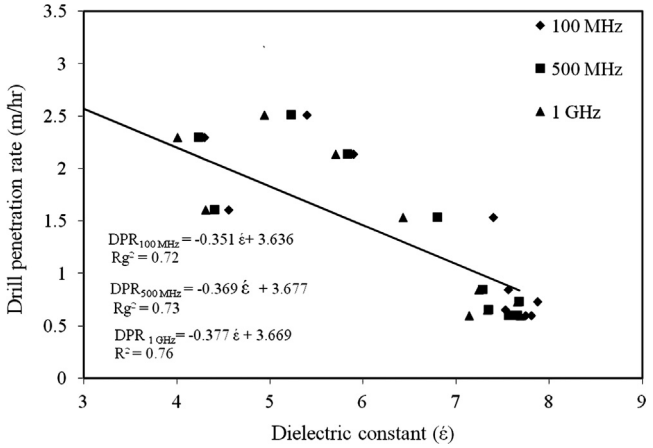

Fig. 4. Calculated drill penetration rate versus the real part of the dielectric constant for desiccated volcanic rock values at 100 MHz, 500 MHz and 1 GHz.

BIS-WTFF, BIS-UTFF, COM-PHOE, and COM-AA can have low dielectric constants and low hardness values; therefore, they have high DPR of between 2 and 2.4 m/h. The other types of basalts (Belleville, NV; Valmont, CO; Somerest, NJ; Pullman, WA; and Saddleback, CA) have high dielectric constants (8.5–10.2) and higher hardness rebound numbers, which correspond to low DPR (0.5–0.8 m/h). The future ExoMars rover will weigh about 700 N on Mars (Brunskill et al., 2011); therefore, a WOB of 350 N (about 50% of the rover weight) will be stable and safe for drilling and sampling the Martian subsurface. Our representation of drill penetration is in showing the importance of the relation between hardness and dielectric and its implication for DPR.

5. Conclusion

We suggest a quantitative method to estimate ground hardness from radar dielectric inversion for drilling and sampling purposes. Radar probing is suggested as a powerful tool to locate regions with highest DPR in the subsurface, based on retrieving low dielectric constant. This approach ensures that future drilling experiments do not miss targets of opportunity such as shallow subsurface volatiles, lose drilling performance, or unnecessarily use power that will be needed for the continuity of the investigation. We conclude that for volcanic surfaces, there is an inverse correlation between DPR based on the rotary-percussive drill method and dielectric constant of volcanic rocks.

Acknowledgments

The authors would like to thank Dr. Valerie Ciarletti from LATMOS, France and Dr. Stephen Clifford from the Lunar and Planetary Institute for their helpful discussion to improve this work. The NASA Planetary Geology and Geophysics Program supported this work under Grants NNXZ08AKA2G and NNG05GL11G. Additional support for PhD graduate student ElShafie was provided by the Arkansas Center for Space and Planetary Sciences, University of Arkansas and the Keck Institute for Space Studies. This research was carried out at the Jet Propulsion Laboratory, California Institute of Technology, under a Contract with the National Aeronautics and Space Administration.

References

Alberti, G., Castaldo, L., Orosei, R., Frigeri, A., Cirillo, G., 2012. Permittivity estimation over Mars by using SHARAD data: the Cerberus Palus area. Journal of Geophysical Research 117 (E9), E09008.

Atkinson, R.H., Bamford, W.E., Broch, E., Deere, D.V., Franklin, J.A., Nieble, C., Rummel, F., Tarkoy, R.J., van Duyse, H., 1978. Suggested methods for determining hardness and abrasiveness of rocks. International Journal of Rock Mechanics and Mining Sciences and Geomechanics 15 (3), 89–98.

Biele, J., 2002. The experiments on board the rosetta lander. Earth, Moon, and Planets 90 (1), 445–458.

Boisson, J., Heggy, E., Clifford, S.M., Yoshikawa, K., Anglade, A., Lognonné, P., 2011. Radar sounding of temperate permafrost in Alaska: analogy to the Martian midlatitude to high-latitude ice-rich terrains. Journal of Geophysical Research 116 (E11), E11003.

Brunskill, Christopher, Nildeep Patel, Thibault P. Gouache, Gregory P. Scott, Chakravarthini M. Saaj, Marcus Matthews, Liang Cui. 2011. Characterisation of martian soil simulants for the ExoMars rover testbed. Journal of Terramechanics 48 (6), 419–438.

Campbell, B.A., Plaut, J.J., Grant, J.A., Freeman, A., 2009. Studying the near-surface Geology of Mars with Imaging Radar. AGU Fall Meeting Abstracts 1, 07.

Ciarletti, V., Corbel, C., Cais, F., Plettemeier, D., Hamran, S.E., Øyan, M., Team, W., 2009. Performances of the WISDOM GPR designed for the shallow sounding of Mars. Lunar and Planetary Institute Science Conference 40, 2367.

Ericson, K., 2004. Geomorphological surfaces of different age and origin in granite landscapes: an evaluation of the Schmidt hammer test. Earth Surface Processes and Landforms 29 (4), 495–509.

Goudie, A.S., 2006. The Schmidt hammer in geomorphological research. Progress in Physical Geography 30 (6), 703.

Gstalder, S., Raynal, J., 1966. Measurement of some mechanical properties of rocks and their relationship to rock drillability. Journal of Petroleum Technology 18 (8), 991–996.

Grimm, R.E., Heggy, E., Clifford, S., Dinwiddie, C., McGinnis, R., Farrell, D., 2006. Absorption and scattering in ground penetrating radar: analysis of the Bishop tuff. Journal of Geophysical Research 111 (E06S02), 15.

Heggy, E., Paillou, P., Ruffié, G., Malezieux, J.M., Costard, F., Grandjean, G., 2001. On water detection in the martian subsurface using sounding radar. Icarus 154 (2), 244–257.

Heggy, E., Paillou, P., Costard, F., Mangold, N., Ruffie, G., Demontoux, F., Malézieux, J.M., 2003. Local geoelectrical models of the martian subsurface for shallow groundwater detection using sounding radars. Journal of Geophysical Research 108 (E4), 8030.

Heggy, E., Clifford, S.M., Grimm, R.E., Dinwiddie, C.L., Wyrick, D.Y., Hill, B.E., 2006. Ground-penetrating radar sounding in mafic lava flows: assessing attenuation and scattering losses in Mars-analog volcanic terrains. Journal of Geophysical Research 111 (E06S04), 16.

Heggy, E., Palmer, E.M., Kofman, W., Clifford, S., Righter, K., Hérique, A., 2012. Radar properties of comets: parametric dielectric modeling of comet 67P/Churyumov–Gerasimenko. Icarus 221, 925–939.

Hucka, V., 1965. A rapid method of determining the strength of rocks in situ. International Journal of Rock Mechanics and Mining Sciences 2, 127–134.

Kahraman, S., Bilgin, N., Feridunoglu, C., 2003. Dominant rock properties affecting the penetration rate of percussive drills. International Journal of Rock Mechanics and Mining Sciences 40, 711–723.

Kofman, W., Safaeinili, A., 2004. Radar techniques applied to subsurface studies in solar system exploration. Tools and Technologies for Future Planetary Exploration 543, 39–50.

Lauretta, D.S., Team, O.R., 2012. An overview of the OSIRIS-REx asteroid sample return mission. Lunar and Planetary Institute Science Conference 43, 2491.

Mouginot, J., Pommerol, A., Beck, P., Kofman, W., Clifford, S.M., 2012. Dielectric map of the Martian northern hemisphere and the nature of plain filling materials. Geophysical Research Letters 39 (2), L02202.

Olhoeft, G.R., Strangway, D.W., 1975. Dielectric properties of the first 100 m of the Moon. Earth and Planetary Science Letters 24, 394–404.

Olhoeft, G.R., 2000. Maximizing the information return from ground penetrating radar. Journal of Applied Geophysics 43 (2), 175–187.

Parkhomenko, E.I., Keller, G.V., 1967. Electrical Properties of Rocks. Plenum Press, New York.

Rust, A.C., Russell, J.K., Knight, R.J., 1999. Dielectric constant as a predictor of porosity in dry volcanic rocks. Journal of Volcanology and Geothermal Research 91, 79–96.

Ulaby, F.T., Bengal, T.H., Dobson, M.C., East, J.R., Garvin, J.B., Evans, D.L., 1990. Microwave dielectric properties of dry rocks. Geoscience and Remote Sensing 28 (3), 325–336.